Study of carbonation rate of synthetic C-S-H by XRD, NMR and FTIR

Wu, Bei; Ye, Guang

Important note
To cite this publication, please use the final published version (if applicable).
Please check the document version above.

Study of carbonation rate of synthetic C-S-H by XRD, NMR and FTIR

Bei Wu [1], Guang Ye [1, 2]

[1] Microlab, Delft University of Technology, the Netherlands

[2] Magnel Laboratory for Concrete Research, Ghent University, Belgium

Supplementary cementitious materials (SCMs) like fly ash (FA) and blast furnace slag (BFS) are broadly used in concrete to replace part of the Ordinary Portland Cement (OPC) because of both economic and environmental issues. In concrete blended with SCMs, C-S-H with different C/S ratios, formed from the hydration and pozzolanic reactions of blended cement, is the major calcium-bearing phases which reacts with CO_2 during carbonation. Therefore, it is important to study the carbonation rate of different C-S-H phases. In this paper, the C-S-H phases (C/S ratio: 0.66 to 2.0) were synthesized and used for accelerated carbonation testing. Synthetic C-S-H phases with different C/S ratios were identified by X-ray diffraction and ^{29}Si nuclear magnetic resonance (NMR). Carbonation rate and products of different C-S-H phases are also determined. The results show that C-S-H (I) phases with different target C/S ratio (lower than 1.40) were synthesized in the mix solution of lime and fume silica. The portlandite appears in the products when the designed C/S ratio is higher than 1.40 under this synthetic condition. C-S-H with lower C/S ratio is decomposed faster than that with a higher C/S ratio. After exposition to the accelerated carbonation condition for three days, in this research, the C-S-H phases with different C/S ratio were all fully decomposed to $CaCO_3$ and silica gel.

Keywords: C-S-H, C/S ratio, structure, carbonation rate

1 Introduction

Carbonation of portlandite (CH) and calcium silicate hydrates (C-S-H) are the main carbonation reactions happened inside the concrete. The consequence is the reduction of alkalinity, which increases the corrosion risk of the reinforcement. Carbonation of CH leads to a reduction of the porosity ascribed to the positive difference of molar volume between CH and $CaCO_3$ (Ngala and Page 1997, Delmi, Aït-Mokhtar et al. 2006), which will slow down the carbonation development in the Ordinary Portland Cement (OPC) concrete. However, the situation will be potentially different in the blended cement concrete.

Supplementary cementitious materials (SCMs) like fly ash (FA) and blast furnace slag (BFS) are broadly used in the concrete to replace parts of OPC because of both economic and environmental issues. Introducing SCMs in the concrete will usually decrease the CH amount in blended cement concrete, caused by the consumption in pozzolanic reactions and dilution effects. Therefore, the major carbonation reaction in blended cement concrete will happen between the C-S-H and CO_2.

Carbonation of C-S-H has been studied by many authors (Šauman 1972, Black, Breen et al. 2007, Morandeau, Thiery et al. 2014). It is a complex decalcification-polymerization process of the C-S-H and the formation of amorphous silica gel, see Eq. (1).

$$C_x SH_y + x\bar{C} \rightarrow xC\bar{C} + SH_t + (y-t)H \tag{1}$$

In which, the cement notations are explained as follows: C = CaO, H = H_2O, S = SiO_2 , A = A_2O_3 , $\bar{C}$ = CO_2 ; x, y and t are the molecular numbers. From the above-mentioned reaction equation, the molar volume change during the carbonation of C-S-H is depended on the properties of C-S-H (like C/S ratio (C/S), water content) and the water remained in silica gel. Unlike the carbonation reaction between CH and CO_2, the volume changes during the carbonation of C-S-H varies among C-S-H phases with different C/S. Therefore, the effect of the C-S-H carbonation on the porosity development is still controversial.

C-S-H phase has a layer structure can be inferred from the refined structure of 11Å tobermorite ($Ca_{4.5}Si_6O_{16}(OH) \cdot 5H_2O$) (Merlino, Bonaccorsi et al. 2001). The layer structure of 11Å tobermorite consists of three parts: CaO_2 sheet, 'dreierkette' form SiO chain and interlayer. In the CaO_2 sheet layer, the 7-fold coordinated Ca^{2+} share all the oxygen atoms with Si^{4+} in SiO chains of SiO_4 tetrahedra on both side of the CaO_2 layer. In the SiO chain layer, SiO_4 tetrahedra coordinate themselves to Ca ions by linking in a dreierketten arrangement, to repeat a kinked pattern after three tetrahedra (Megaw and Kelsey 1956). Two of the tetrahedra are linked to CaO polyhedra by sharing O-O edges with the central Ca-O part of the layer, called paired tetrahedra (PT); the third tetrahedra shares an oxygen atom at the pyramidal apex of a Ca polyhedron, called bridging tetrahedra (BT). There are Ca^{2+} cations and water molecules in the interlayer.

The C/S of C-S-H in the concrete is normally higher than 0.83. The increase of the C/S in C-S-H based on the tobermorite structure can be caused by: omission of the bridging

tetrahedra and incorporation of additional calcium in the interlayer. If all the bridge tetrahedra are removed, the C/S can increase to 1.25 (Taylor and Howison 1956, Richardson 2004). Further incorporation of extra Ca^{2+} in the interlayer can form the C-S-H with a much higher C/S. The theoretical value is 1.50 when all the bridging sites are removed and taken up by extra Ca^{2+} (Richardson 2004). The extra Ca^{2+} is normally balanced by the omission of H^+ or the incorporation of OH^- or both. If the amount of extra Ca continues increasing and achieves a C/S even higher than 1.5, the structure of C-S-H is more close to the C-S-H/CH 'solid solution' (T/CH model) (Richardson 2004).

From the above discussion, three types of Ca exist in the C-S-H structure (classification by the position of Ca): Ca in the CaO_2 sheet layer, Ca in the bridging site and Ca in the interlayer, shown in Figure 1. The proportions of them vary among C-S-H with different C/S ratio. The removal of Ca from the three chemical sites may need different energy, which means the decalcification rate are different among C-S-H phases with different C/S ratio.

The aim of this work is to verify the above-mentioned assumptions, by studying the carbonation rate and products of synthesized C-S-H phases with different C/S and further to explain the phase transformation and microstructure development of blended cement paste during the carbonation, discovered in the previous research (Wu and Ye 2015).
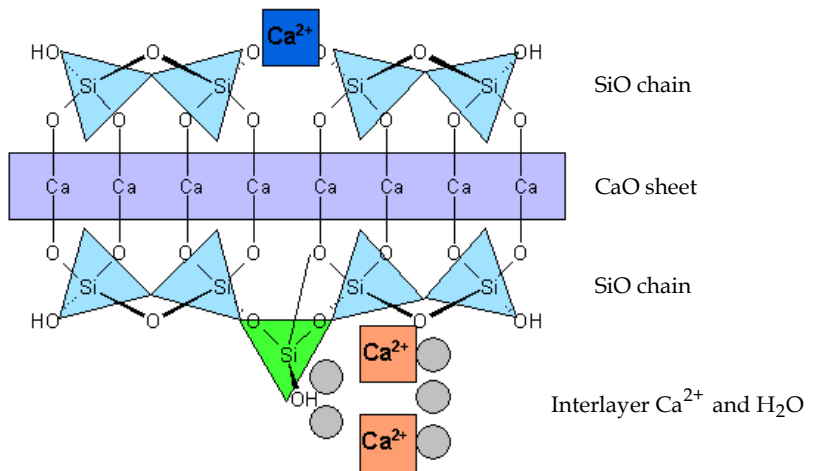

Figure 1: Possible positions of Ca^{2+} in the C-S-H layer structure

2   Experiments and test methods

2.1   Raw Materials

Raw materials used in the synthesis are CaO and fumed silica. CaO is freshly prepared by the calcination of $CaCO_3$ under 1000 °C for at least 4 hours before synthesis. Fumed silica is from Sigma-Aldrich, with the surface area of 175-225 m²/g.

2.2   Synthesis of C-S-H with different C/S

C-S-H gels were prepared by using stoichiometric amounts of CaO and fumed silica, to give approximate C/S ranging between 0.66 and 2.0. The mix design of different C-S-H is described in Table 1. Solid agents were mixed together with CO_2-free water with the water/solid ratio of 50 : 1. The solution was stirred by magnetic stirrer at 20 °C. The whole synthesis procedure was under N2 protection to prevent carbonation. After 2 or 4 weeks of reaction, samples of solid and liquid were extracted as a slurry. Solid products were obtained by filtering the slurries through a Balston No. 45 paper. Then they were quickly moved into the vacuum drying chamber and dried under 35 °C for 24 h. After drying, the samples were stored in the desiccator with the relative humidity of 30%, regulated by the standard saturated $CaCl_2 \cdot 6H_2O$ solution. The set-up of the synthesis device is illustrated in Figure 2.
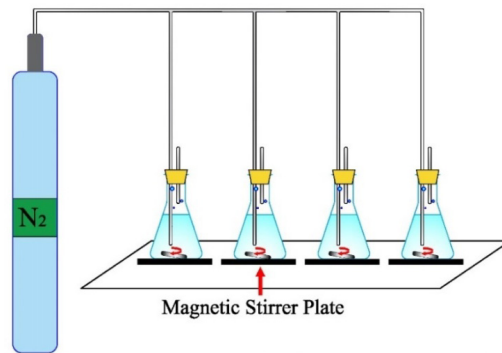

Figure 2: Schematic diagram of the synthesis set-up

2.3   Accelerated carbonation of C-S-H

Well-dried C-S-H samples synthesized for 4 weeks were ground into powders and moved into a carbonation chamber. The CO_2 concentration is maintained at 3% ± 0.2 automatically by the solenoid valve connected with a CO_2 sensor. The temperature is regulated at 20 °C

and the relative humidity is controlled at around 75% by using the saturated NaCl solution. The exposure time varies from 0.5 h to 7 days.

Table 1: Mass fraction of raw materials for preparing different C-S-H

Sample No.	C/S ratio	CaO (g)	SiO_2(g)	H_2O (g)
1	0.66	3.0	4.9	400
2	0.86	3.6	4.4	400
3	1.18	4.2	3.8	400
4	1.40	4.5	3.5	400
5	1.70	4.9	3.1	400
6	2.00	5.2	2.8	400

2.4   *Test methods*

Test methods used for the identification of different types of C-S-H and the carbonation products were X-ray diffraction (XRD), [29]Si nuclear magnetic resonance (NMR) and Fourier transform infrared spectroscopy (FTIR). Before the above-mentioned test, well-dried samples were ground into powders with an average particle size less than 75 µm.

XRD X-ray diffraction (XRD) was used for the identification of different types of C-S-H and the carbonation products. XRD was performed by a Philips PW 1830 diffractometer using CuKa radiation (λ = 0.154056 nm, 60 mA, 40 kV). Two types of scanning were performed on different samples. The first one is the normal scanning with a scan step size of 0.03°, 3 s per step, which was used for analyzing the synthetic products and carbonated products. The second one is the slow scanning with a scan step size of 0.02°, 8 s per step, which was performed on samples used for studying the carbonation rate. Both types of scanning are covering the range from 5° to 70°.

Samples used for studying carbonation rate, were blended with a certain amount of the internal standard corundum (Al_2O_3) (from 12 - 13%wt) and kept inside the sample holder during the carbonation. After each carbonation stage, the sample was taken out with the holder and tested by the XRD slow scanning.

FTIR The FTIR spectra were collected over the wavelength range of 4000 to 400 cm^{-1} by the TM 100 Optical ATR-FTIR spectrometer. The resolution was 4 cm^{-1}.

NMR Solid state ^{29}Si single pulse magic angle spinning (MAS) NMR spectra were acquired using a BrukerMSL-400 spectrometer (magnetic field of 9.8 T; operating frequencies of 79.5 MHz). C-S-H powders were packed into the zirconia rotor sealed at either end with Teflon end plugs and spun at 6 kHz in a Varian 7 mm wide-body probe. The spectra were acquired using a pulse recycle delay of 5 s, a pulse width of 4.97 μs, and an acquisition time of 20 ms; 2002 scans were collected for each sample. ^{29}Si chemical shifts are given relative to tetrakis(trimethylsilyl)silane (TTMSS) at -9.8 ppm, with kaolinite as an external standard at - 91.2 ppm.

3   Results and discussion

3.1   *Synthetic products identification*

3.1.1 XRD

Normal scanning XRD test results of synthetic products are described in Figure 3. The identical peaks with the d-spacing value of 3.04, 2.79, 1.82, 1.66 Å in the pattern indicate that the C-S-H phase synthesized from CaO and fumed silica in the solution is similar to C-S-H (I), which is one of the C-S-H phases found in the Portland cement concrete(Chen, Thomas et al. 2004).

Due to the high reactivity of fumed silica, the C-S-H phases can be formed after 2 weeks' reaction, see Figure 3a. When the designed C/S is less than 1.40, there is only C-S-H phase existing in the product and no trace of unreacted raw materials or carbonation product. However, the portlandite appears when the designed C/S is higher than 1.40 in this research, see Figure 3b. This is consistent with other researchers' results(Garbev, Beuchle et al. 2008, Garbev, Bornefeld et al. 2008, Renaudin, Russias et al. 2009), in which the C-S-H phases are synthesized by using the same method.

3.1.2 NMR

The NMR test results of synthetic products are described in Figure 4a and Figure 4b. The peaks at around -78 ppm and -85 ppm indicates the Q^1 and Q^2 type of tetrahedra respectively (Richardson and Groves 1997) (Cong and Kirkpatrick 1996). Apparently, the intensity of the peak indicating Q^1 increases with increasing of the C/S while the peak intensity of Q^2 decreases.
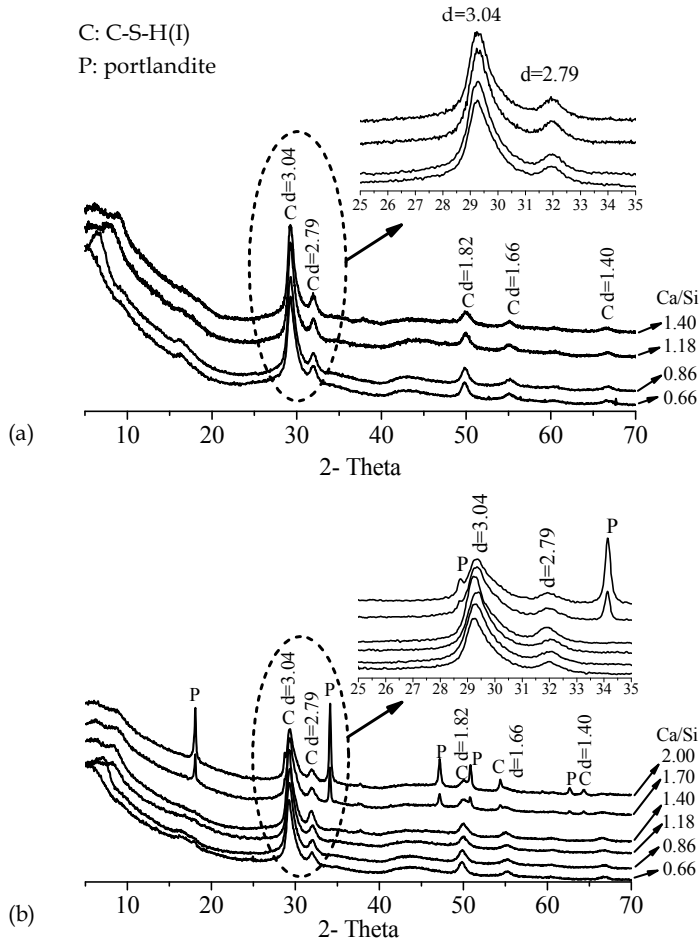
26

Figure 3: XRD test results of C-S-H with different C/S (0.66-2.0). C-S-H d-spacings are noted above their respective peaks in the units of Ångstrom (Å). a-synthesis for 2 weeks; b-synthesis for 4 weeks

The decrease of peak intensity of Q^2 means that the portion of tetrahedra located in the middle of silicate chain decreases. It indicates the breaking of silicate chain and will be followed by the formation of more Q^1 tetrahedra, which can be observed in ^{29}Si NMR spectra as well. Therefore, the mean length of silicate chain will decrease with increasing C/S. Considering the relationship between the mean silicate chain length (MCL) and C/S of C-S-H, the MCL can be used to identify or distinguish C-S-H with different C/S.

The MCL was calculated from the NMR data using Eq. (2) (Richardson 1999) (Richardson and Groves 1992).

27

$$\text{MCL} = \frac{2(Q^1 + Q^2)}{Q^1} \qquad (2)$$

In which, the Q^1 and Q^2 are the fractions of Si present in Q^1 and Q^2 tetrahedra respectively. Quantitative information of the Si fraction was obtained by deconvolution of the single pulse NMR spectra. The spectra were fitted to Gaussian/Lorentzian mixed function (with the ratio of 1.0) using the dmfit2015 software package. An example of the fitting result is illustrated in Figure 5.
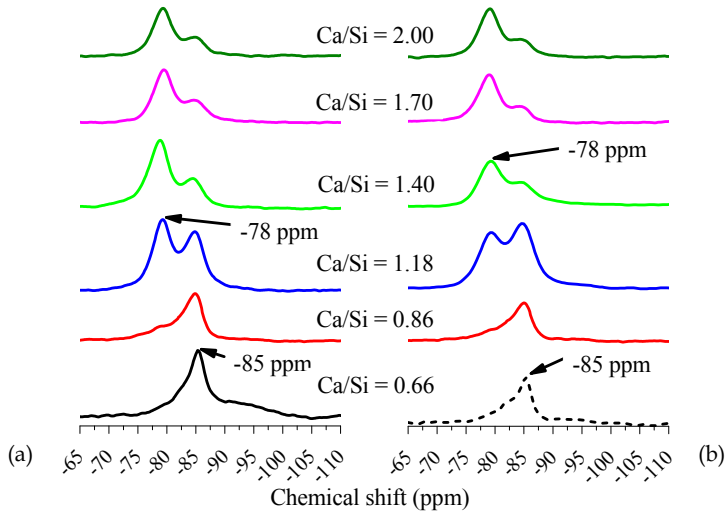

Figure 4: ^{29}Si NMR test results of C-S-H with different C/S (0.66-2.0), a- synthesis for 2 weeks; b-synthesis for 4 weeks

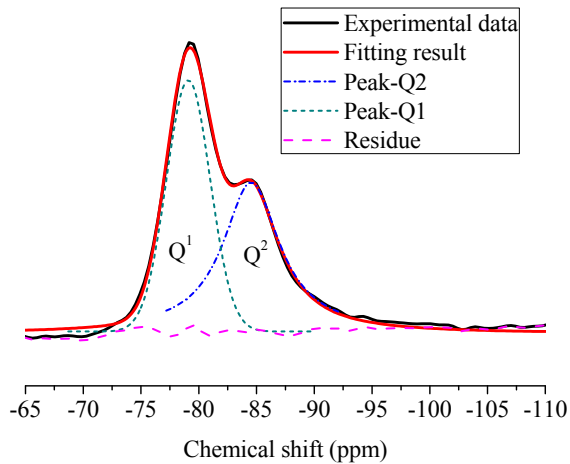*Figure 5: Fitting results of ^{29}Si NMR spectrum (C/S = 1.4, synthesis for 4 weeks)*

28

The deconvolution process is performed on the ^{29}Si NMR test results of synthetic C-S-H with C/S ranging from 0.66 to 2.0. MCL is calculated and plot against the C/S, comparing with the results of C-S-H phases synthesized by the same method (Macphee, Lachowski et al. 1988, Cong and Kirkpatrick 1996, Chen, Thomas et al. 2004, Beaudoin, Raki et al. 2009, He, Lu et al. 2013, L'Hôpital 2014), see Figure 6.
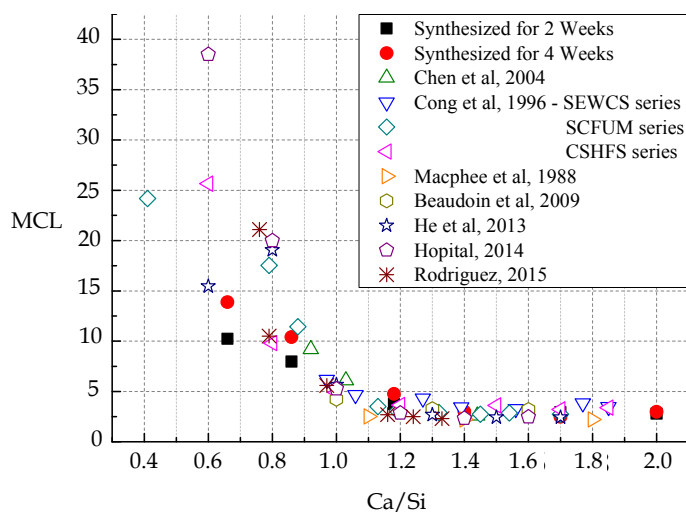

Figure 6: Calculated mean silicate chain length (M CL) of C-S-H with different nominal C/S

The MCL of the C-S-H decreases with the increasing C/S when the C/S is less than 1.4. Then the MCL stays at around 2~3 tetrahedron units long when the C/S increases from 1.4 to 2.0. This can verify the evolution model of C-S-H with higher C/S based on the tobermorite (C/S = 0.83) (Taylor and Howison 1956, Richardson 2004). By omission the bridge tedrahedra, the C/S will increase; meanwhile, the long silicate chain will be broken into shorter polymeric species of SiO4 tetrahedra. Therefore, the MCL of C-S-H decreases with the increase of the C/S. The C/S increases to 1.25 by the omission of all the bridge tetrahedra in the silicate chain. The further incorporation of Ca in the interlayer can achieve the C/S of 1.4, which will not affect the MCL. This is reason that the MCL of C-S-H keeps unchanged when the C/S increases from 1.4 to 2.0.

As the MCL of C-S-H phases has a special relation with the C/S of the C-S-H, this feature is used here to distinguish the C-S-H phases with different C/S. If comparing the data points of this research with the reference data in Figure 6, the C/S of the synthetic C-S-H is

in accord with the initial designed value. Moreover, the XRD test results show only the C-S-H (I) phase. Therefore, the C-S-H phases with different C/S (lower than 1.4) are successfully synthesized in this research. The experiment set-up used in this study can prevent the carbonation effectively.

3.2 *Carbonation of C-S-H with different C/S*

As per the XRD test results, the portlandite appears in the synthetic product and mixes with C-S-H phases when the designed C/S is higher than 1.4. To avoid the effects from the carbonation of portlandite, only the C-S-H with the C/S of 0.66 to 1.40 are used in the accelerated carbonation study. The results are shown and discussed as follows.

3.2.1 NMR

Development of silicate chain in C-S-H with different C/S was studied by ^{29}Si NMR test, shown in Figure 7. These samples were carbonated up to 7 days. In the ^{29}Si NMR spectra, characteristic peaks at around -101 and -111 ppm indicate the Q^3 and Q^4 tetrahedra, respectively. During carbonation, the fraction of Q^3 and Q^4 tetrahedra increases dramatically while the fraction of Q^1 and Q^2 tetrahedra decreases at the same time. This indicate the polymerization process of the silicate chain and the removal of Ca in the CaO_2 sheet layer. The consequence is the linkage of the adjacent silicate chains and to form the silicate network in two and three dimensions. After 7 days' accelerated carbonation, only peaks indicating Q^3 and Q^4 tetrahedra can be observed in the NMR spectra of C-S-H studied. Meanwhile, peaks of Q^1 and Q^2 disappeared. This proves that the final carbonation products of C-S-H is silica gel, not the mixture or 'solid solution' of $CaCO_3$ and C-S-H with lower C/S (Papadakis, Vayenas et al. 1989).

3.2.2 XRD

Slow scanning XRD tests were performed on the C-S-H with the C/S of 0.66, 0.86 and 1.40 to compare the carbonation rate difference. The exposure time varied from 0.5 h to 24 h. The test results are described in Figure 10 to Figure 10.

In the pattern, the major peaks are the characteristic peaks of corundum and C-S-H. And there are nearly no changes of these peaks in the pattern of C-S-H with the C/S of 1.40, during the carbonation. However, in the pattern of C-S-H with the C/S of 0.66 or 0.86, three peaks (2θ = 24.9, 27.0 and 32.8) appear after 1 hour's carbonation, which are the characteristic peaks of μ-$CaCO_3$ (vaterite). Vaterite is one of the three polymorphs of
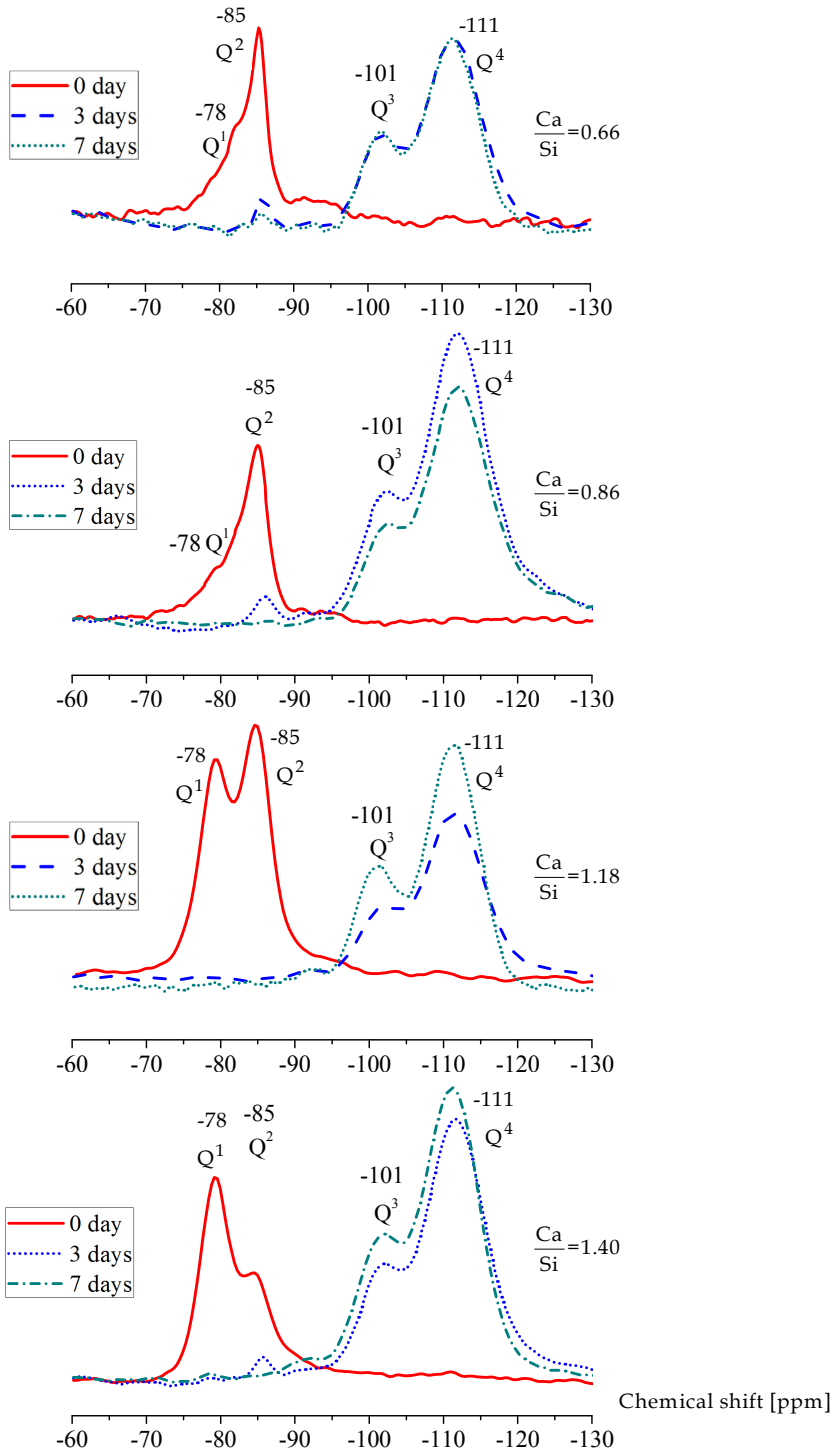
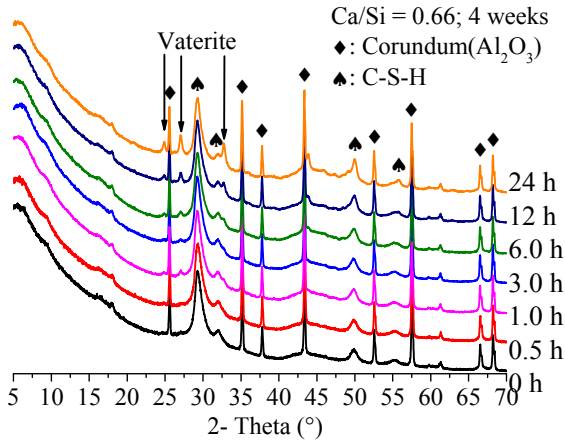*Figure 7: NMR test results of different types of C-S-H, carbonated for different periods*

Figure 8: XRD test results of C-S-H with C/S of 0.66, carbonated for different periods
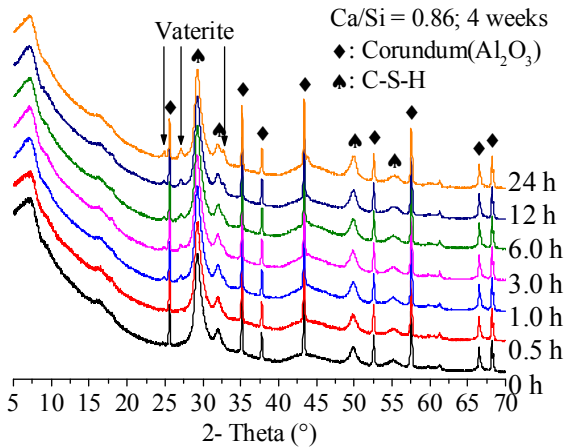

Figure 9: XRD test results of C-S-H with C/S of 0.86, carbonated for different periods
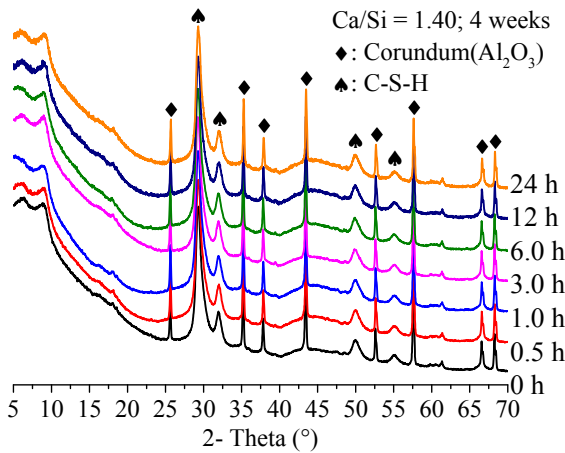

Figure 10: XRD test results of C-S-H with C/S of 1.40, carbonated for different periods

calcium carbonate, the appearance of which indicates the carbonation of C-S-H. Therefore, the carbonation is developed much faster in the C-S-H with lower C/S ratio of 0.66 or 0.86.

3.2.3 FTIR

The FTIR tests were also performed on the carbonated C-S-H samples tested by slow scanning XRD. The test results are compared in Figure 11 to Figure 13 . In the FTIR spectra of C-S-H, peaks at approximate 970 cm-1 and 1066 cm-1 indicate the Si-O stretching vibrations of Q2 tetrahedra. The peak at around 875 and 1400~1500 cm-1 represents the bending (v2) of CO_3^{2-} and the stretching (v3) of CO_3^{2-}, respectively. During carbonation, the peak 1066 cm-1 will grow into an obvious and independent peak. The peak 970 cm-1 will shift to the higher frequency and have a dramatic decrease in the intensity. These changes reveal the progressive polymerization of silicate chains. (McMillan, Wolf et al. 1992, Sykes and Kubicki 1993, Yu, Kirkpatrick et al. 1999). These changes reveal the progressive polymerization of silicate chains. Meanwhile, both peak 875 cm-1 and 1400~1500 cm-1 have a dramatic increase in the intensity, indicating the destruction of silicate chain by the carbonation.

Considering together the changes of above-mentioned peaks (~970 cm-1 and 1066 cm-1), the 'start time' for the carbonation of C-S-H can be observed. This 'critical' time for the C-S-H with the C/S of 0.66, 0.86 and 1.40 are 3h, 6 h and 12 h respectively. Obviously, the C-S-H with a higher C/S is decomposed slower than the C-S-H with lower C/S under the same condition and has a better resistance to the carbonation. This conclusion is in consistent with the XRD test results.

3.2.4 Quantitative information of carbonation rate

Amount of calcium carbonate (vaterite) produced from the carbonation of C-S-H was calculated using Rietveld refinement analysis of XRD spectra showing in Figure 8 and Figure 9. The Rietveld refinement program used is BGMN, realized by the user interface software Profex (Doebelin and Kleeberg 2015). Crystal structure information of vaterite ($CaCO_3$) and Corundum (Al2O3) are imported from the PDF card 04-011-5985 and 00-10-0173. The weight percentage of vaterite was calculated and plotted against the exposure time shown in Figure 14.
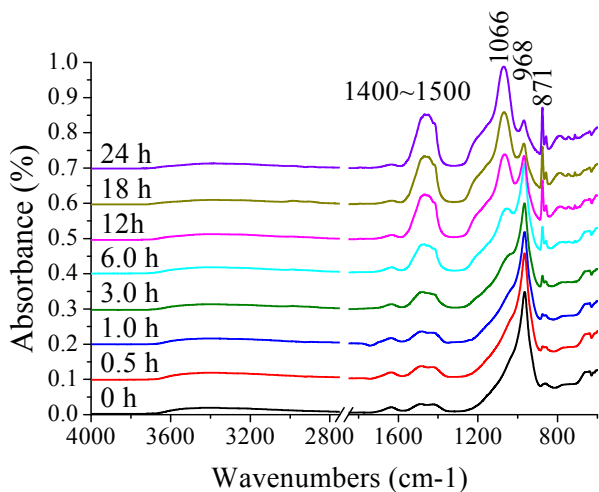
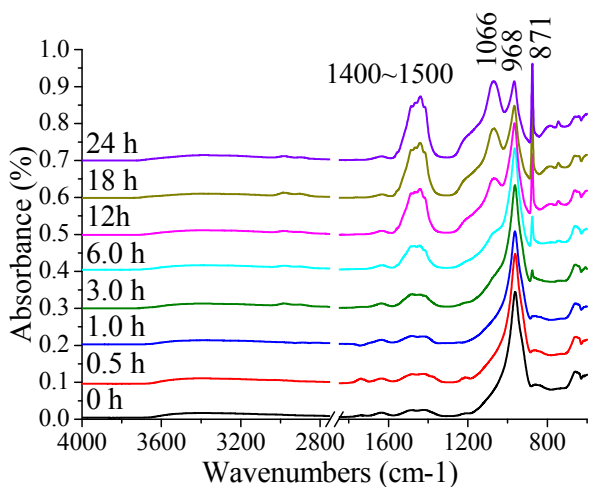*Figure 11: FTIR test results of C-S-H with C/S of 0.66, carbonated for different periods*

Figure 12: FTIR test results of C-S-H with C/S of 0.86, carbonated for different periods
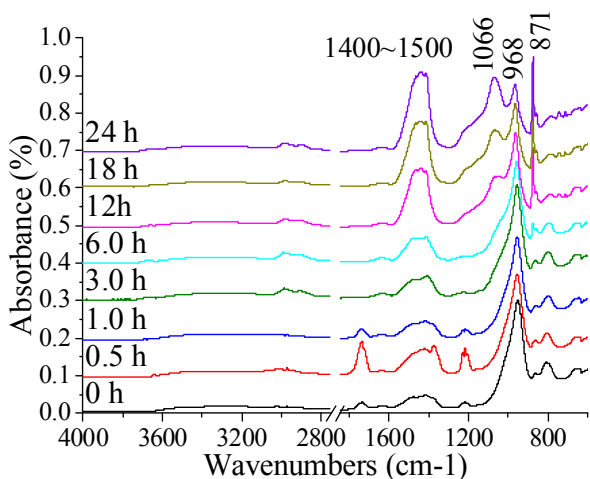

Figure 13: FTIR test results of C-S-H with C/S of 1.40, carbonated for different periods
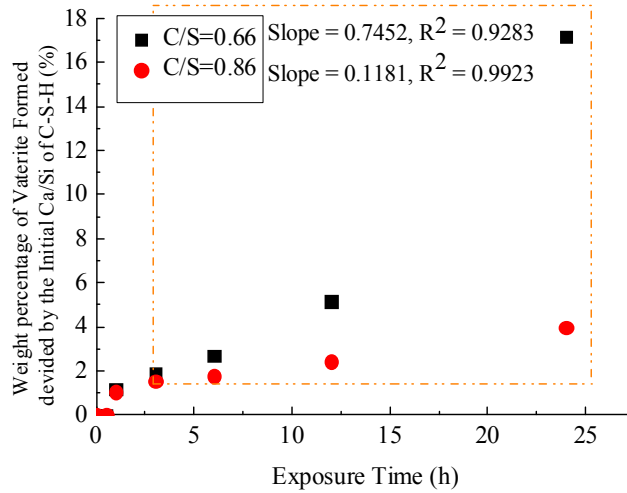
Figure 14: Changes of the weight percentage of calcium carbonate with the exposure time for C-S-H with C/S of 0.66 and 0.86
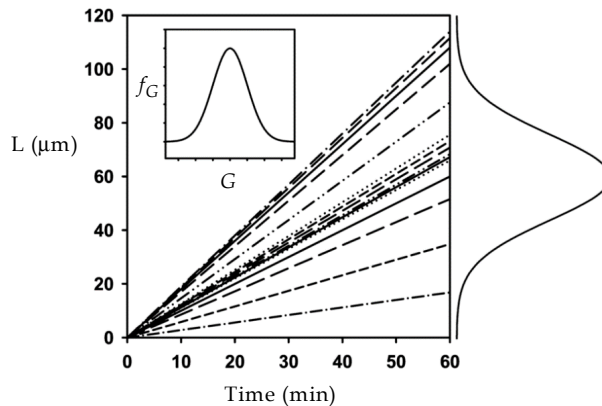

Figure 15: Expected sizes of individual particles in a batch growth cell vs time; the growth rate distribution is shown in the inset, after(Srisanga, Flood et al. 2015)

According to the crystal growth rate dispersion (GRD) model (Srisanga, Flood et al. 2015), which is more accurately describing the variation in the crystal growth rates within a population of crystals, each individual crystal is growing with a unique constant rate. The crystal growth rate dispersion is the assembling of all the growth rates in the population. And the particle size distribution at any time is a linear expansion of the growth rate distribution, shown in Figure 15. Thus, the overall crystal growth rate of the whole population should be a constant as well.

If checking the data points for the exposure time more than 3 hours, the weight percentage of calcium carbonate produced has a linear relation with the exposure time. It means that the growth rate of the carbonate is a constant, which is in consistent with the GRD model. Therefore, the carbonation rate of C-S-H is a constant when considering the longer-time carbonation. Clearly, the carbonation rate of C-S-H with a C/S of 0.66 is higher than that with a C/S of 0.86, which is in consistent with the results found in FTIR test.

4   Conclusions

In the paper, the C-S-H with different C/S, identified by XRD and ^{29}Si NMR, is successfully synthesized from CaO and fumed silica in the solution protected by the N_2 flow. The carbonation mechanism of C-S-H including final products and rate are studied by NMR, FTIR and XRD. The carbonation resistance among different types of C-S-H are discussed. The main conclusions are as follow:

- The C-S-H(I) phases with the C/S ranging from 0.66 to 1.4 were synthesized successfully from CaO and fumed silica in the solution, which is confirmed by different test method. When the designed C/S ratio is higher than 1.40, the portlandite will appear in the synthetic products.

- C-S-H phases with different C/S were all completely decomposed into silicate gel after 3 days' accelerated carbonation in this research. Carbonation rate of C-S-H with a higher C/S is relatively lower than that of C-S-H with lower C/S, which has better resistance to the carbonation.

Literature

Beaudoin, J. J., L. Raki and R. Alizadeh (2009). "A ^{29}Si MAS NMR study of modified C–S–H nanostructures." *Cement and Concrete Composites* 31(8): 585-590.

Black, L., C. Breen, J. Yarwood, K. Garbev, P. Stemmermann and B. Gasharova (2007). "Structural features of C–S–H (I) and its carbonation in air — a Raman spectroscopic study. Part II: carbonated phases." *Journal of the American Ceramic Society* 90(3): 908-917.

Chen, J. J., J. J. Thomas, H. F. Taylor and H. M. Jennings (2004). "Solubility and structure of calcium silicate hydrate." *Cement and Concrete Research* 34(9): 1499-1519.

Cong, X. D. and R. J. Kirkpatrick (1996). "Si-29 MAS NMR study of the structure of calcium silicate hydrate." *Advanced Cement Based Materials* 3(3-4): 144-156.

Delmi, M. M. Y., A. Aït-Mokhtar and O. Amiri (2006). "Modelling the coupled evolution of hydration and porosity of cement-based materials." *Construction and Building Materials* 20(7): 504-514.

Doebelin, N. and R. Kleeberg (2015). "Profex: a graphical user interface for the Rietveld refinement program BGMN." *Journal of applied crystallography* 48(5): 1573-1580.

Garbev, K., G. Beuchle, M. Bornefeld, L. Black and P. Stemmermann (2008). "Cell Dimensions and Composition of Nanocrystalline Calcium Silicate Hydrate Solid Solutions. Part 1: Synchrotron-Based X-Ray Diffraction." *Journal of the American Ceramic Society* 91(9): 3005-3014.

Garbev, K., M. Bornefeld, G. Beuchle and P. Stemmermann (2008). "Cell Dimensions and Composition of Nanocrystalline Calcium Silicate Hydrate Solid Solutions. Part 2: X-Ray and Thermogravimetry Study." *Journal of the American Ceramic Society* 91(9): 3015-3023.

He, Y., L. Lu, L. J. Struble, J. L. Rapp, P. Mondal and S. Hu (2013). "Effect of calcium–silicon ratio on microstructure and nanostructure of calcium silicate hydrate synthesized by reaction of fumed silica and calcium oxide at room temperature." *Materials and Structures:* 1-12.

L'Hôpital, É. M. (2014). *Aluminium and alkali uptake in calcium silicate hydrates (C-S-H)* PhD thesis, EPFL.

Macphee, D., E. Lachowski and F. P. Glasser (1988). "Polymerization effects in CSH: implications for Portland cement hydration." *Advances in Cement Research* 1(3): 131-137.

McMillan, P. F., G. H. Wolf and B. T. Poe (1992). "Vibrational spectroscopy of silicate liquids and glasses." *Chemical Geology* 96(3): 351-366.

Megaw, H. D. and C. H. Kelsey (1956). "Crystal Structure of Tobermorite." *Nature* 177(4504): 390-391.

Merlino, S., E. Bonaccorsi and T. Armbruster (2001). "The real structure of tobermorite 11Å normal and anomalous forms, OD character and polytypic modifications." *European Journal of Mineralogy* 13(3): 577-590.

Morandeau, A., M. Thiery and P. Dangla (2014). "Investigation of the carbonation mechanism of CH and CSH in terms of kinetics, microstructure changes and moisture properties." *Cement and Concrete Research* 56: 153-170.

Ngala, V. T. and C. L. Page (1997). "Effects of carbonation on pore structure and diffusional properties of hydrated cement pastes." *Cement and Concrete Research* 27(7): 995-1007.

Papadakis, V. G., C. G. Vayenas and M. Fardis (1989). "A reaction engineering approach to the problem of concrete carbonation." *AIChE Journal* 35(10): 1639-1650.

Renaudin, G., J. Russias, F. Leroux, F. Frizon and C. Cau-dit-Coumes (2009). "Structural characterization of C–S–H and C–A–S–H samples—Part I: Long-range order investigated by Rietveld analyses." *Journal of Solid State Chemistry* 182(12): 3312-3319.

Richardson, I. (1999). "The nature of CSH in hardened cements." *Cement and Concrete Research* 29(8): 1131-1147.

Richardson, I. (2004). "Tobermorite/jennite-and tobermorite/calcium hydroxide-based models for the structure of CSH: applicability to hardened pastes of tricalcium silicate, β-dicalcium silicate, Portland cement, and blends of Portland cement with blast-furnace slag, metakaolin, or silica fume." *Cement and Concrete Research* 34(9): 1733-1777.

Richardson, I. and G. Groves (1992). "Models for the composition and structure of calcium silicate hydrate (C–S-H) gel in hardened tricalcium silicate pastes." *Cement and Concrete Research* 22(6): 1001-1010.

Richardson, I. and G. Groves (1997). "The structure of the calcium silicate hydrate phases present in hardened pastes of white Portland cement/blast-furnace slag blends." *Journal of Materials Science* 32(18): 4793-4802.

Šauman, Z. k. (1972). "Long-term carbonization of the phases 3CaO. Al_2O_3. $6H_2O$ and 3CaO. Al_2O_3. SiO_2. $4H_2$." *Cement and Concrete Research* 2(4): 435-446.

Srisanga, S., A. E. Flood, S. C. Galbraith, S. Rugmai, S. Soontaranon and J. Ulrich (2015). "Crystal Growth Rate Dispersion versus Size-Dependent Crystal Growth: Appropriate Modeling for Crystallization Processes." *Crystal Growth & Design* 15(5): 2330-2336.

Sykes, D. and J. D. Kubicki (1993). "A model for H_2O solubility mechanisms in albite melts from infrared spectroscopy and molecular orbital calculations." *Geochimica et Cosmochimica Acta* 57(5): 1039-1052.

Taylor, H. and J. Howison (1956). "Relationships between calcium silicates and clay minerals." *Clay Minerals Bull* 3(16): 98-111.

Wu, B. and G. Ye (2015). Development of porosity of cement paste blended with supplementary cementitious materials after carbonation. 14th International Congress on the Chemistry of Cement (ICCC2015).

Yu, P., R. J. Kirkpatrick, B. Poe, P. F. McMillan and X. Cong (1999). "Structure of Calcium Silicate Hydrate (C-S-H): Near-, Mid-, and Far-Infrared Spectroscopy." *Journal of the American Ceramic Society* 82(3): 742-748.